Higgs decay to goldstini and its observability at the LHC

Tao Liu,[1] Lin Wang,[1] and Jin Min Yang[2]

[1]*Institut für Theoretische Teilchenphysik,*
Karlsruhe Institute of Technology (KIT), D-76128 Karlsruhe, Germany
[2]*State Key Laboratory of Theoretical Physics,*
Institute of Theoretical Physics, Academia Sinica, Beijing 100190, China

Abstract

If supersymmetry is broken independently in multiple sectors with different scales, a number of goldstinos will be generated. One linear combination of these goldstinos is massless and eaten by the gravitino, while the orthogonal combinations acquire a tree level mass and become the physical states named goldstini (G'). Compared to the gravitino, such goldstini could couple more strongly to the visible fields and lead to some exotic phenomenology. In this note we first check the goldstini couplings in some GMSB models and find that the goldstini-photon-neutralino interaction may be very small while the goldstini-Z-neutralino and goldstini-Higgs-neutralino interactions may be sizable. This can induce a new decay mode for the Higgs boson: $h \to G' + \chi \to Z + 2G'$. Then we study the observability of this decay channel at the LHC and find that it is not accessible at the finished 8 TeV run (25 fb^{-1}) or 14 TeV run with 100 fb^{-1}, but could be observed at the high luminosity LHC (14 TeV, 1000-3000 fb^{-1}).

PACS numbers: 14.80.Da,14.80.Ly,12.60.Jv

I. INTRODUCTION

Supersymmetry (SUSY) is a consistent extension of Poincare symmetry in quantum field theory and can solve the hierarchy problem in the standard model due to the vanishing of quadratic divergence. However, in a realistic particle theory, SUSY must be broken. Usually it is assumed that SUSY breaking happens in a hidden sector and then is transmitted to low energy fields via certain mechanisms. This will generate a massless goldstino which acts as the longitude component of gravitino in supergravity theory. If SUSY breaking happens in only one sector, the interaction of the gravitino is given by [1, 2]

$$
\begin{aligned}
\mathcal{L}_{int} &= \frac{1}{F}(\partial_\mu G^\alpha J^\mu_\alpha + h.c.), \\
J^\mu &= \sigma^\nu \bar{\sigma}^\mu \psi D_\nu \phi^* - i\sigma^\mu \bar{\psi} F_\phi + i\frac{1}{2\sqrt{2}}\sigma^\nu \bar{\sigma}^\rho \sigma^\mu \bar{\lambda} F_{\nu\rho} + \frac{1}{\sqrt{2}}\sigma^\mu \bar{\lambda} D,
\end{aligned}
\tag{1}
$$

where (ϕ, ψ, F_ϕ) are the boson, fermi and θ^2 components of a chiral superfield; (λ, A_μ, D) are the fermi, gauge and $\theta^2\bar{\theta}^2$ components of a vector superfield; $F_{\nu\rho}$ denotes the strength tensor of the gauge field A_μ and D_μ is the corresponding covariant derivative (throughout this paper we use the two component weyl notation for the fields). The non-derivative couplings can be obtained after integrating by parts and using the equation of motion. From Eq.(1) we see that the gravitino does not play an important role in low energy phenomenology unless the SUSY breaking scale F is sufficiently low.

However, if SUSY is broken in multiple sectors, some exotic phenomenology will be generated [3–11]. In such a scenario, each sector breaks SUSY independently at a scale F_i and gives a goldstino η_i. One linear combination of η_i is massless and eaten by the gravitino, while the orthogonal combinations named goldstinis acquire a tree level mass $m_{G'} = 2m_{3/2}$ in SUGRA [3] (possible loop corrections to the goldstini mass are also considered [3, 8]). The true goldstino (longitudinal component of gravitino) has an interaction in Eq.(1) with $F = \sqrt{\sum_i F_i^2}$. Unconstrained by the supercurrent, the interaction of goldstini can be quite different and large enough to have intriguing phenomenology at colliders. For example, in the framework of gauge mediated SUSY breaking (GMSB), the goldstini can lead to some final states which are softer and more structured at colliders [11]. It can also serve as a dark matter candidate [6]. Additionally, as noted in [9], the goldstini may couple 'strongly' (much stronger than gravitino) with the lightest observable-sector supersymmetric particle (LOSP), which then may lead to some exotic decay channels for the Higgs boson, e.g., the Higgs may decay to the LOSP plus a goldstini.

Given the importance and urgency of Higgs physics, any possible exotic decays of the Higgs boson should be scrutinized. As is well known, a Higgs-like particle around 125 GeV has been observed by ATLAS and CMS collaborations [12, 13], which motivated numerous

theoretical studies, especially the enhanced diphoton decay has been intensively studied in various new physics models, such as the low energy SUSY [14], the little Higgs model [15], the two-Higgs-doublet model [16], the Higgs triplet model [17], the models with extra dimensions [18] and other Higgs extensions [19]. In this note we focus on the effects of goldstini and examine the exotic Higgs decay mode $h \to \chi + G'$ followed by $\chi \to Z + G'$ under the condition $m_Z < m_\chi < m_h$ (here χ is the ordinary lightest neutralino which is assumed to be the LOSP, G' denotes the goldstini).

We will make a brief review on goldstini and explain why we focus on this channel in Section II. Then we take a model-independent way to study the Higgs decay $h \to \chi + G'$ followed by $\chi \to Z + G'$ at the LHC in Section III. Finally, we give our conclusion in Section IV.

II. THEORETICAL MOTIVATIONS

A. A brief review on goldstini

For simplicity we assume that there are only two sequestered sectors which break SUSY spontaneously. Following the arguments in [9], each of them can be parameterized in a non-linear way:

$$X_i = \frac{\eta_i^2}{2F_i} + \sqrt{2}\theta\eta_i + \theta^2 F_i, \tag{2}$$

where η is the so-called goldstino. Due to the non-renormalization theorem of superpotential, visible sector only obtains SUSY breaking information through non-trivial Kähler potential K and gauge kinetic functions f. After integrating out hidden sector fields, X_i couple to single species visible fields Φ as

$$K = \Phi^+\Phi \sum_i \frac{m_{\phi,i}^2}{F_i} X_i^+ X_i, \tag{3}$$

$$f_{ab} = \frac{1}{g_a^2}\delta_{ab}\left(1 + \sum_i \frac{2m_{a,i}}{F_i} X_i\right), \tag{4}$$

where g_a denote the gauge coupling constants, $m_{\phi,a}$ are respectively the soft masses for the scalar of the chiral superfield and gauginos. The trilinear and bilinear soft terms between multiple fields could also be constructed, but since they are subleading and model-dependent in the contribution to interactions between goldstino and visible sector, we do not consider them here. Substituting the expression of X_i into the above formula gives the Lagrangian

up to order $1/F_i$:

$$
\begin{aligned}
\mathcal{L} = &- \sum_i m_{\phi,i}^2 \phi^* \phi + \sum_i \frac{m_{\phi,i}^2}{F_i} \eta_i \psi \phi^* \\
&- \frac{1}{2} \sum_i m_{a,i} \lambda^a \lambda^a - \sum_i \frac{i m_{a,i}}{\sqrt{2} F_i} \eta_i \sigma^{\mu\nu} \lambda^a F_{\mu\nu}^a + \sum_i \frac{m_{a,i}}{\sqrt{2} F_i} \eta_i \lambda^a D^a .
\end{aligned}
\tag{5}
$$

The mass eigenstates can be obtained by a rotation of η_i:

$$
G = \cos\theta \eta_1 + \sin\theta \eta_2, \quad G' = -\sin\theta \eta_1 + \cos\theta \eta_2,
\tag{6}
$$

where θ is defined by $\tan\theta = F_2/F_1$. It is easy to see that the Weyl spinor G is related to SUSY breaking scale $F = \sqrt{F_1^2 + F_2^2}$ while G' vanish in the non-linear form. Then the interaction Lagrangian becomes

$$
\mathcal{L}_G = \frac{m_\phi^2}{F} G \psi \phi^* - \frac{i m_a}{\sqrt{2} F} G \sigma^{\mu\nu} \lambda^a F_{\mu\nu}^a + \frac{m_a}{F} G \lambda^a D^a,
\tag{7}
$$

$$
\mathcal{L}_{G'} = \frac{\tilde{m}_\phi^2}{F} G' \psi \phi^* - \frac{i \tilde{m}_a}{\sqrt{2} F} G' \sigma^{\mu\nu} \lambda^a F_{\mu\nu}^a + \frac{\tilde{m}_a}{F} G' \lambda^a D^a,
\tag{8}
$$

with the parameter m and $\tilde{m}$ defined as

$$
m_{\phi/a} = m_{\phi/a,1} + m_{\phi/a,2}, \quad \tilde{m}_{\phi/a} = -m_{\phi/a,1} \tan\theta + m_{\phi/a,2} \cot\theta.
\tag{9}
$$

$\mathcal{L}_G$ is just the non-derivative version of Eq.(1) and the couplings are proportional to the soft masses as expected. For goldstinis, their interactions with visible fields could be enhanced as long as $\tilde{m}$ is larger than m. Note that if D^a get a vacuum expectation value, there will be small mixing between λ^a and η_i. In most cases this mixing is very small, so we can omit it safely.

The mass of goldstini is given at tree level by $m_{G'} = 2 m_{3/2}$ due to the intrinsic property of SUGRA. Additionally, there could be corrections to such a tree-level mass, which, however, are model-dependent [3, 8]. In our analysis we assume that both m_G and $m_{G'}$ are very smaller than the Higgs mass.

B. Couplings between goldstini and Higgs boson

Without the extra goldstinis, the interaction of goldstino (G) with the lightest neutralino (χ) is given by

$$
\mathcal{L} = \frac{y_1}{\sqrt{2} F} \chi G h + \frac{y_2}{2\sqrt{2} F} \chi \sigma^{\mu\nu} G F_{\mu\nu}^\gamma + \frac{y_3}{2\sqrt{2} F} \chi \sigma^{\mu\nu} G Z_{\mu\nu} + \frac{y_4}{\sqrt{2} F} \bar{\chi} \bar{\sigma}^\mu G Z_\mu + h.c.
\tag{10}
$$

where $F^\gamma_{\mu\nu}$ is the photon field strength, Z_μ and $Z_{\mu\nu}$ are respectively the Z-boson field and its field strength. In the minimal supersymmetric standard model (MSSM), the above parameters $y_{1,2,3,4}$ are given by

$$y_1 = -N_{11}^{-1}m_1 m_Z \sin\theta_W \sin(\alpha+\beta) + N_{21}^{-1}m_2 m_Z \cos\theta_W \sin(\alpha+\beta)$$
$$+N_{31}^{-1}(B_\mu \cos\alpha - m_{H_d}^2 \sin\alpha) + N_{41}^{-1}(-B_\mu \sin\alpha + m_{H_u}^2 \cos\alpha), \tag{11}$$

$$y_2 = -2im_\chi(N_{11}^* \cos\theta_W + N_{12}^* \sin\theta_W), \tag{12}$$

$$y_3 = -2im_\chi(-N_{11}^* \sin\theta_W + N_{12}^* \cos\theta_W) - 2im_Z(N_{13}^* \cos\beta - N_{14}^* \sin\beta), \tag{13}$$

$$y_4 = im_Z^2(-N_{11}^* \sin\theta_W + N_{12}^* \cos\theta_W) + im_Z m_\chi(N_{13}^* \cos\beta - N_{14}^* \sin\beta). \tag{14}$$

where N_{1i} denote the mixing between the lightest neutralino and the gauginos or higgsinos. We see that unless the SUSY breaking scale F is small enough, such interactions of goldstino could hardly affect the 125 GeV Higgs.

Naively speaking, the interactions of the goldstini can be obtained from the above expression with the goldstino G replaced by the goldstini G' and each soft mass replaced by its corresponding $\tilde{m}$. Then it is clear that for $\tilde{m} \gg m$ the interactions of the goldstini can be significantly stronger than the goldstino. However, there are some subtle differences which deserve attention.

Next, let us scrutinize the concrete low energy interactions of the goldstini. The first one is its interaction with Higgs and neutralino: $\frac{\tilde{y}_1}{\sqrt{2}F}\chi G'h$. From Eq.(8) we can obtain the coefficient of this interaction:

$$\tilde{y}_1 = -N_{11}^{-1}\tilde{m}_1 m_Z \sin\theta_W \sin(\alpha+\beta) + N_{21}^{-1}\tilde{m}_2 m_Z \cos\theta_W \sin(\alpha+\beta)$$
$$+N_{31}^{-1}(\tilde{B}_\mu \cos\alpha - \tilde{m}_{H_d}^2 \sin\alpha) + N_{41}^{-1}(-\tilde{B}_\mu \sin\alpha + \tilde{m}_{H_u}^2 \cos\alpha). \tag{15}$$

Similarly, the interaction with photon and neutralino takes a form of $\frac{\tilde{y}_2}{2\sqrt{2}F}\chi\sigma^{\mu\nu}G'F^\gamma_{\mu\nu}$ with

$$\tilde{y}_2 = -2im_\chi\left[\frac{\tilde{m}_1}{m_1}N_{11}^* \cos\theta_W + \frac{\tilde{m}_2}{m_2}N_{12}^* \sin\theta_W\right]. \tag{16}$$

The interaction with Z-boson and neutralino is somewhat complicated. But based on the experience obtained above, some hints could be obtained. From the expression of $y_{3/4}$, it can be easily found that the Z-boson can be divided into two parts: one is its transverse component proportional to $(-N_{11}^* \sin\theta_W + N_{12}^* \cos\theta_W)$, and the other is the longitude component proportional to $(N_{13}^* \cos\beta - N_{14}^* \sin\beta)$. The interaction of goldstini with the transverse part of the Z-boson is almost the same as photon because they come from the same origin $\frac{im_{a,i}}{\sqrt{2}F_i}\eta_i\sigma^{\mu\nu}\lambda^a F^a_{\mu\nu}$. After multiplying a factor $\tilde{m}_1/m_1$ to $N_{11}^* \cos\theta_W$ and a factor $\tilde{m}_2/m_2$ to $N_{12}^* \sin\theta_W$ in Eqs.(13,14), we can get the coefficient of this transverse coupling. For the longitude component of the Z-boson, since it has some relations with the tilded mass parameters of the Higgs, such as $\tilde{m}_{h_{u,d}}$ and $\tilde{\mu}$, we can not get the same simple result. In [11]

a free factor K_{Z_L} is introduced to connect the longitudinal interaction between G and G'. Although we do not know the exact formula for K_{Z_L}, it must be a function of $\tilde{m}_\phi/m_\phi$ from naive arguments and dimensional analysis (here m_ϕ denotes the soft Higgs parameters). The details of the coupling between Z-boson and goldstini can be found in the appendix of [9].

From the above analysis we see that the $G' - \gamma - \chi$ coupling is proportional to $\tilde{m}_a$ (tilded gaugino masses) while the $G' - Z - \chi$ and $G' - h - \chi$ couplings are proportional to $\tilde{m}_{a,\phi}$. So, if $\tilde{m}_a$ are very small while $\tilde{m}_\phi/m_\phi$ is much larger than one, we can get a new scenario in which the Higgs decay $h \to \chi G' \to Z G' G'$ is more sizable than $h \to \chi G' \to \gamma G' G'$. Note that from the viewpoint of model-building, this scenario could be easily realized in a two-sector messenger with $F_1 \gg F_2$. If the second sector preserves R-symmetry, it will give no contribution to the gaugino masses. Besides, in some concrete GMSB models, especially the direct gauge mediation [21], the gaugino masses are usually suppressed by a factor F_i^2/M_i^4 due to the vacuum structure of superfields. So it is common to have approximately vanishing $\tilde{m}_a$. Additionally, in the case of stimulate SUSY breaking [22], it is quite natural to split F_1 and F_2.

III. HIGGS DECAY TO GOLDSTINI AT THE LHC

From the analysis in the preceding section, we see that in some GMSB models the goldstini couplings $G' - h - \chi$ and $G' - Z - \chi$ can be sizable while the coupling $G' - \gamma - \chi$ can be much suppressed. This scenario can lead to the Higgs decay $h \to \chi G' \to Z G' G'$ which will be studied in this section.

A. The rate of Higgs decay to goldstini

We take an effective way to study the Higgs decay $h \to \chi G' \to Z G' G'$. The effective Lagrangian is given by

$$\mathcal{L}_{eff} = \frac{m^2}{F}[g_{h\chi} h \chi G' + \frac{g_{\chi Z_1}}{m} G' \sigma^{\mu\nu} Z_{\mu\nu} \chi + g_{\chi Z_2} \bar{G}' \bar{\sigma}^\mu Z_\mu \chi + h.c.] \qquad (17)$$

Here a mass parameter m is introduced to make the couplings $g_{h\chi}$, $g_{\chi Z_1}$ and $g_{\chi Z_2}$ dimensionless and the Lagrangian takes the similar form as in [23] which studied the signal of monophoton plus missing energy from the Higgs decay. Note that for $m_\chi > m_h$, the lightest neutralino can decay to the Higgs boson which may lead to many boosted Higgs bosons at the LHC [24].

For the Higgs decay $h \to Z G' G'$, if it proceeds through an off-shell neutralino, i.e., $h \to \chi^* G' \to Z G' G'$, its rate is small. But if the neutralino can be on-shell, the decay

$h \to \chi G' \to Z G' G'$ may be sizable. In Fig. 1 we show the partial widths for $h \to Z G' G'$ and $\chi \to Z G'$. We see that only for an on-shell neutralino (lighter than the Higgs boson and heavier than the Z-boson) can the decay $h \to Z G' G'$ be sizable.
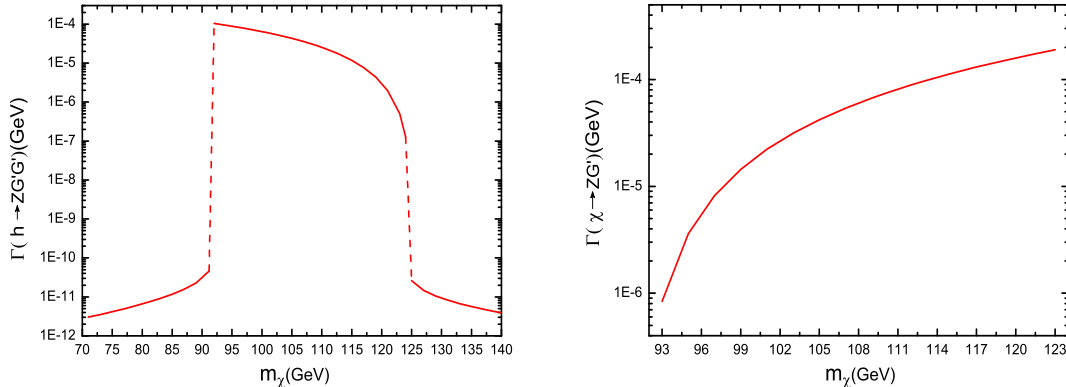

FIG. 1: The partial widths of $h \to Z G' G'$ and $\chi \to Z G'$ versus the neutralino mass. Here we choose $m = 0.1\sqrt{F}$ with $\sqrt{F} = 1.5$ TeV, and $g_{h\chi} = g_{\chi Z_1} = g_{\chi Z_2} = 1$.

Note that there are already some constraints on the whole SUSY breaking scale $\sqrt{F}$ through the interaction of gravitino (usually photon is also involved). The current lower bound is around 300 GeV [25, 26] and it is expected that the LHC could push it to about 1.6 TeV [27]. The most sensitive process to $\sqrt{F}$ is the decay channel $h \to \chi G'$ whose branching ratio is proportional to $1/F$. In our calculation we fix $\sqrt{F} = 1.5$ TeV and $m = 0.1\sqrt{F}$, and assume all the dimensionless couplings to be unity.

About the decay of the neutralino χ, it may have some other modes, e.g., decay to SM particles if R-parity is violated or decay to a light $U(1)_X$ gaugino [28]. In our calculation we assume that χ only decays to $Z G'$. If there are other decay modes, the corresponding signal should be multiplied by the branching ratio $Br(\chi \to Z G')$. Additionally, the decay length of the nuetralino with energy E is approximately $\Gamma^{-1}\sqrt{(E^2 - m_\chi^2)/m_\chi^2} \sim 10^{-10} cm$, so the neutralino will decay inside the detector.

B.   Signal and background

With the goldstini couplings in Eq.(17), the final state $Z G' G'$ can come from three processes at the LHC, as shown in Fig. 2. Generally, the processes (a) and (b) will generate Z-boson with low transverse momentum, while (c) with t-channel squark exchange may generate a Z-boson with large transverse momentum [27]. Additionally, heavier squarks which are consistent with the result of LHC will suppress the t-channel contributions, so we will not consider the process (c).
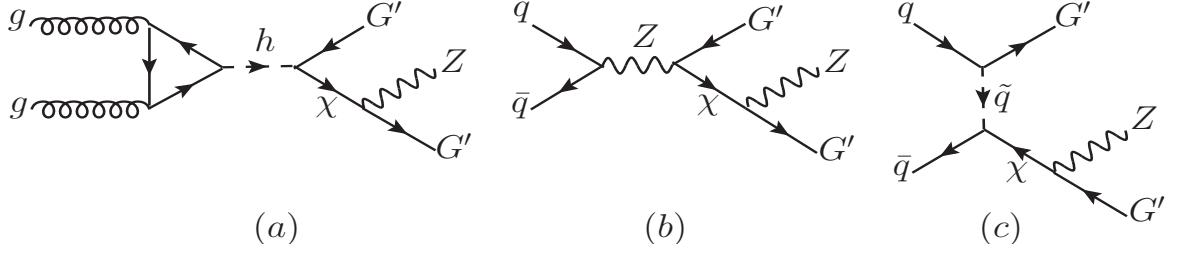
7

FIG. 2: Feynman diagrams for the production of $ZG'G'$ at the LHC induced by the goldstini couplings in Eq. (17).

We require the Z-boson produced in association with goldstini to decay to electrons or muons. Therefore, the signal is a pair of electrons or muons and low missing transverse momentum, i.e., $pp \to Z + \not{E}_t \to l^+l^- + \not{E}_t$ ($l = e, \mu$). Some studies about such mono-Z process have been performed in [29–31], where the mono-Z has a large transverse momentum. In our signal, the Z-boson has small transverse momentum because it comes from the decay of the neutralino.

For the s-channel process shown in Fig.2(a), the Higgs boson can be produced on-shell and then decay to the Z-boson plus missing energy. For such a production we can get the high order corrections by multiplying a k-factor. At the LHC, the leading order Higgs boson production in the SM is from the gluon-gluon fusion. We calculate the Higgs boson production cross section at $\sqrt{s} = 14$ TeV with CTEQ6M parton distribution functions. We set the renormalization scale μ_R and factorization scale μ_F at the Higgs mass of 125 GeV. The other relevant parameters are set as

$$m_t = 173.3 \text{ GeV}, \quad m_b = 4.67 \text{ GeV}, \quad m_Z = 91.188 \text{ GeV}, \quad m_W = 80.4 \text{ GeV} \qquad (18)$$

We consider the higher order corrections and follow [23] to get $\sigma_h^{NNLO} = 49.99$ pb at the next-to-next-to leading order with next-to-next-to leading logarithm resummation.

For the Z-boson s-channel process shown in Fig.2(b), the neutralino can be produced on-shell and then decay to Z-boson and G'. So far no high order corrections have been calculated for this process and we calculate this production at the leading order.

The main SM backgrounds are

$$pp \to ZZ \to l^+l^-\nu\bar{\nu}, \qquad (19)$$

$$pp \to W^+W^- \to l^+\nu l^-\bar{\nu}, \qquad (20)$$

$$pp \to Zj \to l^+l^-j, \qquad (21)$$

$$pp \to t\bar{t} \to b\bar{b}l^+l^-\nu\bar{\nu}, \qquad (22)$$

$$pp \to ZW^\pm \to l^+l^-l^\pm\nu. \qquad (23)$$

TABLE I: The number of signal and background events for the LHC with $\sqrt{s} = 14$ TeV and 10 fb^{-1} of integrated luminosity.

$\sqrt{s} = 14$ TeV $(10fb^{-1})$	Background (B)				Signal (S)		
	$ZZ \to l^+l^-\nu\bar{\nu}$	$W^+W^- \to l^+\nu l^-\bar{\nu}$	$Zj \to l^+l^-j$	B_{tot}	S_h	S_Z	S_{tot}
no cut	964	12598	37950	51512	72	21	93
$\|m_{ll} - m_Z\| < 5$ GeV	834	900	33000	34734	58	18	76
$\not{E}_T < 30$ GeV	133	214	20700	21047	58	4	62

Obviously, the first two processes are our backgrounds. Because they proceed through the electroweak interaction, their cross sections are expected to be relatively small at the LHC. The third process can mimic our signal with the missing jet, which happens for $|\eta_j| > 4$ [23]. For the forth process to mimic our signal, the two b-jets must be missing, which is less likely. So we will not consider it. For the last process, one lepton must be missing, similar to the third process. Since its cross section is much smaller than the third process, we neglect it in our calculation. Therefore, in our analysis we only consider the first three processes. In our calculation we use MadGraph5 [20] for both the signal and background.

C. Numerical results

Before giving the numerical result on the signal and backgrounds, we summarize our selection criteria on the final state:

$$P_T^l > 20 \ GeV, \quad \not{E}_T > 20 \ GeV, \quad |\eta_l| < 2.5, \quad |\eta_j| > 4.0, \quad \Delta R \equiv \sqrt{\Delta\eta^2 + \Delta\phi^2} > 0.4, \ (24)$$

where the separation ΔR is for the leptons or jet in the final state with $\Delta\eta$ being the pseudo-rapidity difference and $\Delta\phi$ being the azimuthal angle difference. In Table I we present the number of events for the LHC with $\sqrt{s} = 14$ TeV and 10 fb^{-1} of integrated luminosity. In our calculation of the signal, the mass parameters in Eq. (17) are fixed as $m_\chi = 110$ GeV, $m_{G'} = 0$ (the goldstini is much lighter than the Higgs, so we set it to zero for simplicity), $m = 0.1\sqrt{F}$, $\sqrt{F} = 1.5$ TeV, while all the dimensionless couplings are fixed to unity.

From Table I we see that the signal is overwhelmed by the backgrounds. The largest background is from $Z + jet$ production, which is about three orders above the signal. As expected, the cut on the invariant dilepton mass $|m_{ll} - m_Z| < 5$ GeV can suppress the W^+W^- background efficiently. Since in our signal the missing transverse momentum is relatively low, the cut on the missing E_T can further suppress the backgrounds.

Finally, we show in Table II the signal significance for different integrated luminosity. Since the contribution from the s-channel Z-boson process is much smaller than the Higgs

TABLE II: Same as Table I, but showing the event number of the signal $pp \rightarrow h \rightarrow \chi G' \rightarrow ZG'G' \rightarrow l^+l^- + E_t$ and its significance for the LHC with $\sqrt{S} = 14$ TeV and different luminosity.

$\sqrt{S} = 14$ TeV	100 fb^{-1}	500 fb^{-1}	800 fb^{-1}	1000 fb^{-1}	2000 fb^{-1}	3000 fb^{-1}
$S_{[no\ cut]}$	720	3600	5760	7200	14400	21600
$S_{[passing\ all\ cut]}$	580	2900	4640	5800	11600	17400
$S/\sqrt{S+B}$	1.3	2.8	3.6	4.0	5.6	7.0

process (as shown in Table I), in Table II we only consider the Higgs process so that the result could be interpreted as the product of the Higgs production rate, the Higgs decay branching ratio and the neutralino decay branching ratio. We see that only for the high luminosity LHC with 1000-3000 fb^{-1} can the signal be observable.

IV. CONCLUSION

Compared with the gravitino, the goldstini can couple more strongly to the visible fields and thus induce some interesting phenomenology. In this note we considered the effects of the goldstini on the Higgs phenomenology. We found that in some GMSB models the goldstini has approximately vanishing interaction with photon and the lightest neutralino, but the corresponding coupling with the Z-boson is sizable. This could induce the mono-Z decay of the Higgs boson ($h \rightarrow G' + \chi \rightarrow Z + 2G'$) which signals mono-Z and missing E_t at the LHC. Then in an effective model we studied the observability of this decay at the LHC. From a Monte Carlo simulation of the signal and background, we found that it is not accessible at the finished 8 TeV run (25 fb^{-1}) or 14 TeV run with 100 fb^{-1}, but could be observed at the high luminosity LHC (14 TeV, 1000-3000 fb^{-1}). Although at the LHC it is so challenging to detect this exotic decay channel of the Higgs boson, it is worth hunting because such a scenario may naturally exist in GMSB with multi SUSY breaking sectors.

---

[1] P. Fayet, Phys. Lett. B **70**, 461 (1977).

[2] H. K. Dreiner, H. E. Haber and S. P. Martin, Phys. Rept. **494**, 1 (2010).

[3] C. Cheung, Y. Nomura and J. Thaler, JHEP **1003**, 073 (2010).

[4] C. Cheung, J. Mardon, Y. Nomura and J. Thaler, JHEP **1007**, 035 (2010).

[5] N. Craig, J. March-Russell and M. McCullough, JHEP **1010**, 095 (2010).

[6] H. -C. Cheng, W. -C. Huang, I. Low and A. Menon, JHEP **1103**, 019 (2011).

[7] K. Mawatari and Y. Takaesu, Eur. Phys. J. C **71**, 1640 (2011).

[8] R. Argurio, Z. Komargodski and A. Mariotti, Phys. Rev. Lett. **107**, 061601 (2011).

[9] J. Thaler and Z. Thomas, JHEP **1107**, 060 (2011).

[10] C. Cheung, F. D'Eramo and J. Thaler, JHEP **1108**, 115 (2011).

[11] R. Argurio *et al.*, JHEP **1206**, 096 (2012).

[12] G. Aad *et al.* [ATLAS Collaboration], Phys. Lett. B **716**, 1 (2012).

[13] S. Chatrchyan *et al.* [CMS Collaboration], Phys. Lett. B **716**, 30 (2012).

[14] M. Carena *et al.* JHEP 1203, 014 (2012); JHEP **1207**, 175 (2012); J. Cao *et al.*, JHEP **1203**, 086 (2012); JHEP **1210**, 079 (2012); Phys. Lett. B **710**, 665 (2012); Phys. Lett. B **703**, 462 (2011); arXiv:1301.4641; U. Ellwanger, JHEP 1203, 044 (2012); U. Ellwanger, C. Hugonie, arXiv:1203.5048; A. Arbey *et al.*, JHEP **1209**, 107 (2012); K. Hagiwara, J. S. Lee, J. Nakamura, JHEP 1210, 002 (2012); R. Benbrik *et al.*, arXiv:1207.1096; N. Christensen, T. Han, S. Su, arXiv:1203.3207; T. Cheng, arXiv:1207.6392; B. Kyae, J.-C. Park, arXiv:1207.3126; H. An, T. Liu, L.-T. Wang, arXiv:1207.2473; J. F. Gunion, Y. Jiang and S. Kraml, arXiv:1207.1545; J. Ke *et al.*, arXiv:1207.0990; G. Belanger *et al.*, arXiv:1208.4952; M. Drees, arXiv:1210.6507; S. F. King *et al.*, arXiv:1211.5074; K. Choi *et al.*, arXiv:1211.0875; M. Berg *et al.*, arXiv:1212.5009; L. Aparicio *et al.*, arXiv:1212.4808; C. Balazs, S. K. Gupta, arXiv:1212.1708; K. Cheung, C.-T. Lu, T.-C. Yuan, arXiv:1212.1288; A. Chakraborty *et al.*, arXiv:1301.2745;

[15] J. Reuter, M. Tonini, arXiv:1212.5930; X.-F. Han *et al.*, arXiv:1301.0090; L. Wang J. M. Yang, Phys. Rev. D **84**, 075024 (2011); Phys. Rev. D **79**, 055013 (2009).

[16] C. Haluch, R. Matheus, Phys. Rev. D **85**, 095016 (2012); X.-G. He, B. Ren, J. Tandean, Phys. Rev. D **85**, 093019 (2012); A. Arhrib, R. Benbrik, C.-H. Chen, arXiv:1205.5536; E. Cervero and J.-M. Gerard, arXiv:1202.1973; L. Wang, X.-F. Han, JHEP **1205**, 088 (2012); A. Drozd *et al.*, arXiv:1211.3580; S. Chang *et al.*, arXiv:1210.3439; N. Chen, H.-J. He, JHEP **1204**, 062 (2012); T. Abe, N. Chen, H.-J. He, arXiv:1207.4103; C. Han *et al.*, arXiv:1212.6728.

[17] A. G. Akeroyd, S. Moretti, Phys. Rev. D **86**, 035015 (2012); A. Arhrib *et al.*, JHEP **1204**, 136 (2012); L. Wang, X.-F. Han, Phys. Rev. D **86**, 095007 (2012); Phys. Rev. D **87**, 015015 (2013).

[18] G. Blanger *et al.*, arXiv:1201.5582; K. Cheung, T.-C. Yuan, Phys. Rev. Lett. **108**, 141602 (2012).

[19] Y. Cai, W. Chao, S. Yang, arXiv:1208.3949; S. Chang *et al.*, arXiv:1207.0493; J. Berger, J. Hubisz, M. Perelstein, JHEP **1207**, 016 (2012); S. Dawson, E. Furlan, Phys. Rev. D **86**, 015021 (2012); S. Dawson, E. Furlan, I. Lewis, arXiv:1210.6663; M. Chala, arXiv:1210.6208; C. -S. Chen *et al.*, arXiv:1301.4694.

[20] J. Alwall *et al.*, JHEP **1106**, 128 (2011).

[21] Z. Komargodski and D. Shih, JHEP **0904**, 093 (2009).

[22] M. McCullough, Phys. Rev. D **82**, 115016 (2010).

[23] C. Petersson, A. Romagnoni and R. Torre, JHEP **1210**, 016 (2012).

[24] K. Howe and P. Saraswat, JHEP **1210**, 065 (2012).

[25] D. Acosta *et al.* [CDF Collaboration], Phys. Rev. Lett. **89**, 281801 (2002).

[26] P. Achard *et al.* [L3 Collaboration], Phys. Lett. B **587**, 16 (2004).

[27] A. Brignole, F. Feruglio, M. L. Mangano and F. Zwirner, Nucl. Phys. B **526**, 136 (1998).

[28] M. Baryakhtar, N. Craig and K. Van Tilburg, JHEP **1207**, 164 (2012).

[29] F. J. Petriello, S. Quackenbush and K. M. Zurek, Phys. Rev. D **77**, 115020 (2008).

[30] N. F. Bell *et al.*, Phys. Rev. D **86**, 096011 (2012).

[31] L. M. Carpenter, A. Nelson, C. Shimmin, T. M. P. Tait and D. Whiteson, arXiv:1212.3352.